The AERosol and TRACe gas Collector (AERTRACC): an online measurement controlled sampler for source-resolved emission analysis

5 Julia Pikmann[1], Lasse Moormann[1], Frank Drewnick[1], Stephan Borrmann[1,2]

[1]Particle Chemistry Department, Max Planck Institute for Chemistry, Mainz, 55128, Germany
[2]Institute for Atmospheric Physics, Johannes Gutenberg University Mainz, Mainz, 55128, Germany

Correspondence to: Frank Drewnick (frank.drewnick@mpic.de)

Abstract.

10 Probing sources of atmospheric pollution in complex environments often leads to the measurement and sampling of a mixture of different aerosols due to fluctuations of the emissions or the atmospheric transport situation. Here, we present the AERosol and TRACe gas Collector (AERTRACC), a system for sampling various aerosols independently on separate sampling media, controlled by parallel online measurements of particle, trace gas, and meteorological variables, like particle number or mass concentration, particle composition, trace gas concentration as well as wind direction and speed. 15 AERTRACC is incorporated into our mobile laboratory (MoLa) which houses online instruments measuring various physical and chemical aerosol properties as well as trace gas concentrations. Based on preparatory online measurements with the whole MoLa setup, suitable parameters measured by these instruments are used to define individual sampling conditions for each targeted aerosol using a dedicated software interface. Through evaluation of continuously online measured data with regard to the sampling conditions, the sampler automatically switches between sampling and non-sampling for each of up to 20 four samples, which can be collected in parallel. Particle and gas phase of each aerosol, e.g. source emissions and background, are sampled onto separate filters (PM_1 and PM_{10}) and thermal desorption tubes, respectively. Information on chemical compounds in the sampled aerosol is accomplished by thermal desorption chemical ionization mass spectrometry (TD-CIMS). The design, operation, and characterization of the sampler are presented. For in-field validation, wood-fired pizza oven emissions were sampled as targeted emissions separately from ambient background. Results show that the 25 combination of well-chosen sampling conditions allows more efficient and effective separation of source-related aerosols from the background, as seen by increases of particle number and mass concentration and concentration of organic aerosol types, with minimized loss of sampling time, compared to alternative sampling strategies.

1 Introduction

Atmospheric aerosol changes radiative forcing, alters cloud formation and precipitation, and affects human health. Within 30 multiphase processes aerosol interacts with atmospheric gases forming new substances (Fuzzi et al., 2015; Johnston and Kerecman, 2019; Shrivastava et al., 2017). Still the impact of these effects on climate and health are not sufficiently well

understood as aerosol sources, composition, properties, and transformations are poorly characterized (Parshintsev and Hyötyläinen, 2015).

Atmospheric aerosol can originate from diverse sources, natural as well as anthropogenic ones. Particles can be emitted
35 directly as primary emissions from combustion processes of fossil fuel and biomass as well as in the form of biological emissions like bacteria and pollen. Furthermore, secondary aerosol forms through gas-to-particle conversion by oxidation processes in the atmosphere (Celik et al., 2020; Fuzzi et al., 2015; Gordon et al., 2017; Struckmeier et al., 2016). Depending on the surroundings, different types of emissions and the background aerosol can blend into complex mixtures, complicating the identification of the contribution by the original emissions sources.

40 Atmospheric aerosol consists of two major chemical fractions, the inorganic one with substances like ammonium, nitrate, sulfate, metal oxides, mineral dust, and sea salt (Fuzzi et al., 2015), while the organic aerosol, the other fraction, constitutes the more complex part. Especially fine particulate matter, which has a relevant effect on climate and health, contains usually a large organic fraction. These particles consist of many individual components but only a small fraction of them are identified by state-of-the-art instruments (Fuzzi et al., 2015; Johnston and Kerecman, 2019; Zhou et al., 2020). The analysis
45 and identification of these organic components is necessary for better understanding of chemical processes, transport, sources, and particle formation in the atmosphere. This knowledge is crucial to improve existing models and facilitate prediction of climate effects (Johnston and Kerecman, 2019; Zhou et al., 2020).

Because of the broad variety of species, the characterization of organic aerosol is demanding and therefore numerous techniques for aerosol analysis have been developed (Forbes, 2020; Johnston and Kerecman, 2019). Techniques for analysis
50 and characterization of aerosols are classified into two main categories, online and offline techniques. Offline measuring techniques frequently provide detailed information about different aerosol properties based on separate sampling and analysis (Parshintsev and Hyötyläinen, 2015). For chemical analysis, this approach offers the possibility to use all available analysis techniques to get detailed information at the expense of low time and particle size resolution (Hallquist et al., 2009; Heard, 2006). A broad variety of techniques are available for chemical analysis. Techniques like ICP-MS (inductively
55 coupled plasma mass spectrometry) and XRF (x-ray fluorescence) provide information about the elemental composition of the sample (Bhowmik et al., 2022; Ebert et al., 2016), while FTIR (Fourier-transform infrared spectroscopy) and NMR (nuclear magnetic resonance spectroscopy) are used to determine organic functional groups in aerosols (Faber et al., 2017; Gilardoni, 2017). For identification of individual species, techniques with separation prior to detection are applied. Widely used for this purpose are GC-MS (gas chromatography mass spectrometry) and HPLC-MS (high performance liquid
60 chromatography mass spectrometry); however they are typically only able to identify a relatively small fraction of the whole organic aerosol (Forbes, 2020). Single particle techniques like SIMS (secondary ion mass spectrometry) and SEM (scanning electron microscope) provide information about the elemental composition and its distribution as well as information about the particle morphology (Bai et al., 2018; Laskin et al., 2018).

To obtain data with high time resolution online and semi-online techniques are used. With these techniques, samples are
65 analyzed continuously or semi-continuously without the need of additional a-posteriori laboratory work as for offline

techniques. One of the most widely used methods for aerosol online analysis is aerosol mass spectrometry (AMS) measuring the single particle or particle ensemble chemical composition of submicron particles. While offering real-time data due to short acquisition intervals it lacks detailed chemical information, lost through fragmentation during vaporization and ionization (Canagaratna et al., 2007). Consequently, identification of individual organic components is rarely possible

70 (Hallquist et al., 2009). A semi-continuous online bulk analysis can be performed with the thermal-optical EC/OC analyzer measuring the hourly concentrations of elemental carbon (EC) and organic carbon (OC). Other semi-continuous systems like PILS (particle into liquid sampler) and MARGA (monitor for aerosols and gases in ambient air) sample the water-soluble aerosol fraction followed by subsequent analysis with e.g. ion chromatography (Stavroulas et al., 2019; Zhou et al., 2015). More comprehensive analysis is achieved with TAG (thermal desorption aerosol gas chromatography) (Williams et al.,

75 2006) and FIGAERO-CIMS (filter inlet for gas and aerosols chemical ionization mass spectrometry) (Lopez-Hilfiker et al., 2014), which sample aerosol for several tens of minutes and analyze the samples after automated thermal desorption. These semi-continuous techniques offer rather detailed information on the organic aerosol fraction due to low fragmentation. However, with time resolutions of tens of minutes up to an hour, characterization of transient emissions or disentanglement of aerosol blends in environments affected by several sources is not feasible. Currently, no instrument offers detailed

80 chemical analysis of aerosols in real-time for the analysis of individual sources (Parshintsev and Hyötyläinen, 2015).

To comprehensively analyze and characterize individual sources in complex environments like cities or industrial areas, where fluctuating meteorological and atmospheric transport conditions result in mixing of emissions from different sources, or transient source emissions like from ships, aircrafts or short-term processes, identification of individual species on short time scales is necessary. Since offline methods or highly species-resolving semi-online methods do not provide the required

85 temporal resolution and quick online methods do not provide in-depth chemical analysis capability for such applications, we developed the AERosol and TRACe gas Collector (AERTRACC), which combines the advantages of both approaches. AERTRACC collects samples of different aerosols on separate sampling media for subsequent in-depth chemical analysis. Separation of aerosols is hereby achieved by controlling the sampling process with high-time resolution online measurements. AERTRACC is integrated in our mobile aerosol research laboratory (MoLa), a vehicle equipped with online

90 measuring instruments (Drewnick et al., 2012), serving as control unit for the sampler via a tailor-made software interface. There the user can define sampling conditions based on measured parameters like particle number concentration or wind direction to separately collect the different aerosols. The analysis of the samples is performed with TD-HR-ToF-CIMS (thermal desorption high resolution time-of-flight chemical-ionization mass spectrometry) offering high resolution mass spectra combined with high sensitivity and low sample fragmentation as well as minimized sample preparation effort

95 (Aljawhary et al., 2013; Mercier et al., 2012; Yatavelli et al., 2012). Here, we present the design and characteristics of AERTRACC and demonstrate its capabilities in a field experiment, probing a pizza oven in a semi-urban environment.

2 Design and operation of the AERTRACC sampling system

2.1 The mobile aerosol research laboratory (MoLa)

The mobile laboratory MoLa houses the newly developed AERTRACC sampling system and serves as data-providing basis
for its control unit. MoLa is designed for mobile and stationary measurements of ambient air composition and is mainly used
for characterization of source specific emissions (Drewnick et al., 2012; Fachinger et al., 2021). A variety of online
instruments measures different aerosol and meteorological properties providing high time resolution data of seconds until
one-minute averaging intervals. This includes physical particle properties, e.g. particle number size distributions, as well as
chemical characterization like the non-refractory chemical composition of submicron particles, and trace gas concentrations
of various gases as NO_x, O_3, and CO_2. An overview of the MoLa instruments and measured variables, which are used to
control the AERTRACC system, is provided in Table 1; for further description see Drewnick et al. (2012). Stationary
measurements can be performed with the sampling inlet at different heights (3-10 m above ground level) using an inlet setup
on MoLa's roof.

Table 1: MoLa instruments used for control of the AERTRACC sampler.

Instrument	Measured variables	Particle diameter range	Time resolution
Aethalometer[a]	Black and brown carbon mass concentration	< 1.0 µm	1 s
PAS[b]	Polyaromatic hydrocarbon mass concentration on particle surface	10 nm - 1 µm	12 s
EDM[c]	PM_1, $PM_{2.5}$, PM_{10} mass concentration based on optical measured size distribution	0.25 - 10 µm	6 s
CPC[d]	Particle number concentration	5 nm - 3 µm	1 s
OPC[e]	Particle size distribution based on optical diameter	0.25 - 32 µm	6 s
Airpointer[f]	Mixing ratio of CO, SO_2, O_3. NO_x	-	4 s
NO_2/NO/NO_x Monitor[g]	Mixing ratio of NO_2, NO, NO_x	-	5 s
LICOR[h]	Mixing ratio of CO_2. H_2O	-	1 s
Meteorological Station[i]	Wind direction, wind speed, relative humidity, temperature, rain intensity, pressure	-	1 s
GPS[j]	Location	-	1s

[a]Magee Scientific Aethalometer® Model AE33, Magee Scientific, USA. [b]Photoelectric Aerosol Sensor PAS2000, EcoChem Analytics, USA.
[c]Environmental Dust Monitor EDM180, Grimm Aerosoltechnik, Germany. [d]Condensation Particle Counter Model 3786, TSI, Inc., USA. [e]Optical Particle
Counter Model 1.109, Grimm Aerosoltechnik, Germany. [f]AirPointer, Recordum Messtechnik GmbH, Austria. [g]NO2/NO/NOx Monitor Model 405 nm, 2B
Technologies, Inc., USA. [h]LI840, LI-COR, Inc., USA. [i]WXT520, Vaisala, Finland. [j]Navilock NL-8022MU, Navilock, Germany.

2.2 Setup of the AERTRACC sampling system

AERTRACC is designed to sample different aerosol types separately on individual sample carriers. The system is incorporated in MoLa with its own inlet and a flow path designed for minimal particle losses, minimizing non-vertical tubes and bends. With four available sampling paths up to four different aerosols can be sampled separately. It is possible to 120 sample particles up to 10 µm in aerodynamic diameter (PM_{10}) and up to 1 µm (PM_1) on quartz fiber or PTFE filters as well as volatile compounds onto thermal desorption tubes (TDT) filled with adsorbent material (further details in Sect. 2.4). To accomplish separate sampling of different aerosol types based on the MoLa online data a control software for the AERTRACC sampler was programmed (see Sect. 2.3).

A schematic overview and a photograph of the sampling system installed in MoLa are shown in Fig. 1. The AERTRACC 125 sampler has its own inlet line (ID = 48 mm), equipped with a PM_{10} inlet head (Digitel, Switzerland, inlet flow rate 30 L min^{-1}), which is mounted on the roof of MoLa. The inlet is located 0.5 m apart from the MoLa online instrument inlet and their heights are adjusted to each other to assure sampling of the same aerosol.
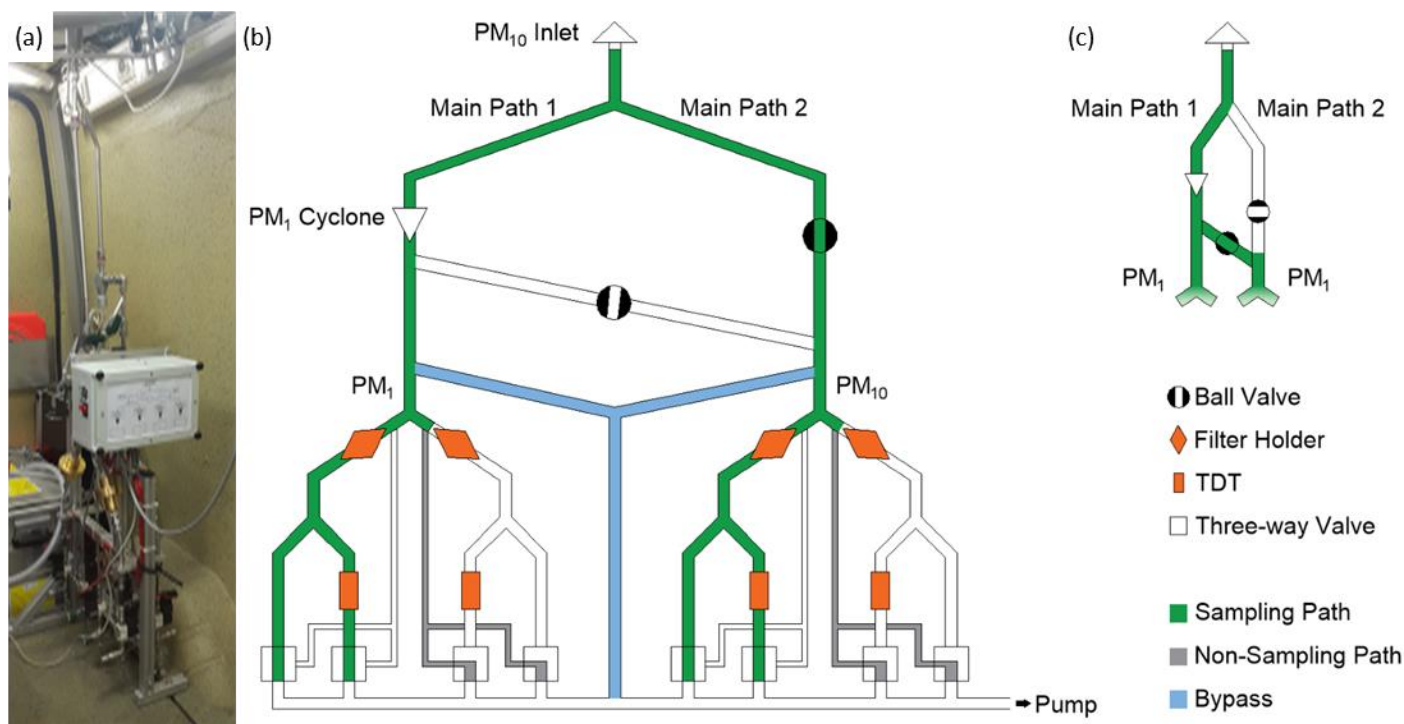
130 **Figure 1: Photo (a) and scheme (b+c) of the AERTRACC sampler with active flow paths marked in green for sampling flows, in grey for non-sampling flows, and in blue for bypass flows (b: sampling mode PM_1+PM_{10}, c: sampling mode PM_1 only). Needle and dosing valves are located in each path directly upstream of the pump and are not shown in the scheme.**

Inside MoLa the inlet tube is split into two main paths, which are both split again, in total into four sampling paths. Main path 1 (see Fig. 1b) contains a PM_1 cyclone (URG, USA, flow rate 16.7 L min^{-1}). Downstream the cyclone, main path 1 is connected with main path 2 with a cross tube. With two ball valves, one installed in main path 2 and the other one in the cross tube between the main paths, the user can sample in two different sampling modes. Either two sampling paths are used for PM_{10} and the other two for PM_1 (Fig. 1b; cross tube not used) or all four sampling paths are used for PM_1 sampling (Fig. 1c; cross tube used to feed also main path 2 through the cyclone).

Each of the four sampling paths contains a custom-made filter holder made of gold-coated aluminum for filters of 25 mm diameter and a TDT. The sampling area on the filters equals the thermal desorption area for the subsequent analysis. The operation flow rate for filter sampling is limited to 4.2 or 7.5 L min^{-1} (¼ of 16.7 or 30 L min^{-1}) due to the required flow rates for the PM_1 cyclone or the PM_{10} inlet, depending on the chosen sampling mode (see above). Behind each filter holder, the sampling line splits again into a path with TDT and a TDT bypass path. This split is necessary, as the flow rate through the TDT has to be smaller (typically limited to 0.2 L min^{-1}) than the one through the filter to avoid a loss of the retention volume for the gaseous species. The described active sampling paths are shown in Fig. 1b as green paths. The flows through the filter holders are the sum of the flows through the respective TDT and TDT bypass lines. Simple and quick change of filter holders and TDTs is achieved with Ultra-Torr vacuum fittings (Swagelok Company, USA) before and behind each device.

To assure a permanent air flow through the whole system, independent whether a certain sample line is active or not, a non-sampling path around the sampling media is added in parallel to each sampling line (grey paths in Fig. 1b are the active non-sampling paths). The flow through the sampling system is switched between sampling and non-sampling path using magnetic three-way valves (SMC, VT307, Japan) and maintained by a rotary vane pump (V-VTE 10, Gardner Denver, Inc., USA). This permanent air flow through the system keeps the cut-offs of the size selectors and the transport losses constant and allows the targeted aerosol to be sampled almost immediately as soon as the respective three-way valve is switched when the evaluation of the online data shows that the sampling conditions are fulfilled. The adjustment of flow rates for the sampling paths is achieved with precision dosing valves (HF-1300-SS-L-1/4-S, Hamlet, Germany) for the TDT flow rates and with needle valves (Nupro SS-4HS V51, Swagelok, USA) for the additional flow through the filters. To adjust the flows through the two main paths to match the specified flow rates through the inlet head and the cyclone, independent of the individual sample line flow rates, an additional bypass line is split from each main path (blue paths in Fig. 1b). These bypass lines are directly connected to the pump via additional needle valves. The sampling line and bypass tubing are made of stainless steel with tube diameters of 1/2" upstream the filter holders and 1/4" after the filter holders.

The AERTRACC electronics including the control of the magnetic valves via a custom-made relay card and relays is housed in an electronic box attached to the sampler (white box in Fig. 1a). The front of the box contains an LED status display showing which sampling path is active. The relay card is connected via RS232 to the MoLa data acquisition computer, which collects the online instruments data.

2.3 Control software and sampler operation

The AERTRACC control software (ACS) is the interface between the MoLa online measurements and the sampling system and is integrated into the MoLa data acquisition software for simple and direct access to the data. In the ACS, the user defines criteria for sampling up to four different aerosols separately, based on measured MoLa online data. The software

170 continuously evaluates the incoming online data whether the criteria for sampling are fulfilled and controls the flow through the individual sampling paths accordingly. For effective and user-friendly operation, a graphical user interface (Fig. 2) was programmed where the user selects the sampling conditions for the targeted aerosols and obtains real-time information on the sampling process, such as the accumulated sampling time and estimated collected mass on the filters. In the upper part of the main ACS window, the user chooses the operation and sampling mode. The lower part is divided into four boxes, one for

175 each sampling path, where the user can set sampling conditions individually for each path.

The two available sampling modes for AERTRACC are either all four sampling paths collecting PM_1 aerosol or two pairs of sampling paths collecting PM_1 and PM_{10}, respectively, using the same sampling conditions for each pair. When changing between the sampling modes the user needs to switch the ball valves of the cross tube accordingly (see Fig. 1b+c).

The user can choose between two operation modes. The sampler can either be operated in *automatic mode* with user defined

180 sampling conditions (Fig. 2a), which are based on variables, measured by the MoLa online instruments, or in *manual mode* (Fig. S3), where the user can directly start and stop sampling with the additional possibility to pre-select the collection time or collected mass on the filters. The total collected mass on the filters is calculated based on the EDM online mass concentration data, measured during the actual sampling intervals, and the respective filter flow rate.

In the *automatic mode* the user defines individual sampling conditions for each sampling path (Fig. 2a). Each sampling

185 condition consists of up to four criteria, which can be logically combined using the Boolean operators AND, NOT, and OR. Individual criteria are fulfilled if the value of the selected parameter, e.g. a particle or trace gas concentration, but also time, GPS location, meteorological condition, or total collected mass, is between the user-selected minimum and maximum values. This allows complex definitions of sampling conditions for each of the targeted aerosols. A possible scenario, based on recent MoLa measurements (Fachinger et al., 2021), could be measuring with MoLa at a place where traffic and biomass

190 burning emissions can be measured depending on the wind direction. Using suitable sampling conditions, both types of emissions could be sampled separately. For the biomass burning aerosol the sampling condition could be "suitable wind direction range AND high black carbon concentration AND high PM_1 concentration"; while for the traffic aerosol the sampling condition could be "suitable wind direction range AND high particle number concentration AND NOT high PM_1 concentration". For background aerosol sampling the mentioned variables should be accordingly set to low concentrations

195 and the remaining wind direction sections.

The *flowrate* sub-window contains information on the flow setup of the AERTRACC sampler (Fig. 2b). Here, the user enters the flow rates, which are adjusted with the individual needle valves. The graphical user interface automatically provides the combined flow rates at critical devices, such as the inlet cyclone, and thus supports the correct selection of the individual

flow rates in order to match their required flow conditions. Furthermore, in this window the MoLa inlet height is entered.
200 This information is used to select the correct delay times between registration of the sampling status, i.e. sampling or non-sampling, and the activation or de-activation of flows through the individual sampling paths (see Sect. 3.2).

When the sampling path is activated, the software continuously compares the chosen sampling conditions with the actual measured online data. For visual support a colored indicator shows for each sampling path whether sampling (green) or no sampling (red) takes place or the sampling path is inactive (grey). Depending on whether the sampling conditions for a

205 certain sampling path are fulfilled, the respective three-way valves are switched accordingly between sampling path and non-sampling path via the relay card. For each sampling path, two displays in the ACS show the current accumulated collection time and sampled aerosol mass. A data logger automatically keeps track of all activities performed by the user on the interface and of all sampling periods, which are logged with the time stamp, type of activity and respective sampling conditions.

210
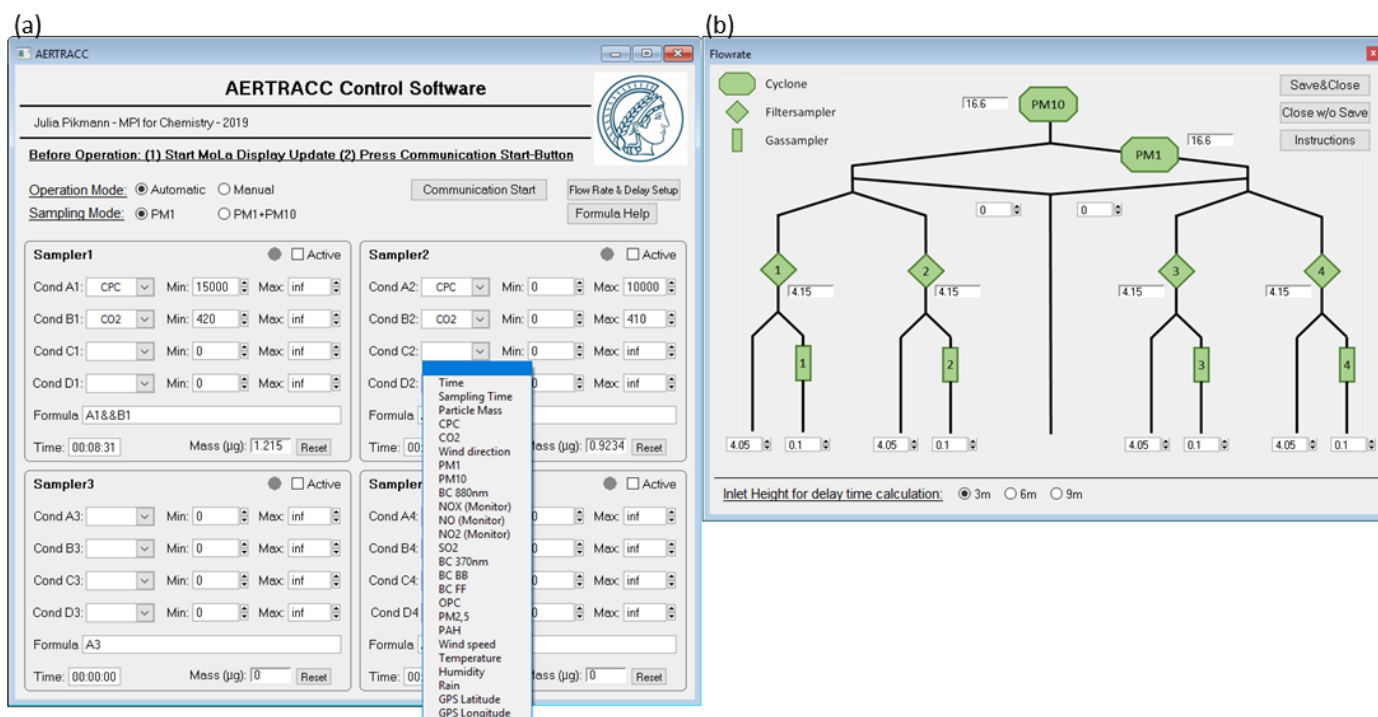
Figure 2: User interface of the AERTRACC software with main window (a) and flowrate sub-window (b).

2.4 Sampling media

The choice of the sampling media was based on the selection of thermal desorption as sample introduction method for the
215 subsequent analysis using TD-CIMS, which reduces the chances of potential contamination through sample preparation. For gas phase sampling, TDTs were used, made of stainless steel (1/4" OD, 89 mm length) and packed with Tenax TA (MS Wil, Netherlands) and Carbograph 5TD (Markes International Ltd., United Kingdom), each 150 mg. Together, these adsorbents

are applicable to compounds with a broad volatility range (mainly $C_4 - C_{32}$) to investigate different kinds of emissions. They were also chosen as they are hydrophobic, inert and temperature stable up to 350 °C, necessary for the high temperature during thermal desorption (Dettmer and Engewald, 2002, 2003; Harper, 2000; Woolfenden, 2010). Before sampling, TDTs were conditioned in a TC-20 conditioner (Markes International Ltd., United Kingdom) at 300 °C for 4 hours with nitrogen (purity 99.9999%, 0.09 L min^{-1}).

For particle sampling, PTFE filters with 25 mm diameter (Type 11803, Sartorius, Germany) were used, which were pre-baked at 200 °C under vacuum (50 hPa) for 24 h before sampling.

Typical sampling flow rates are usually between 1 and 8 L min^{-1} for the filter samples, with mass loadings not exceeding 2 µg to avoid overloading the CIMS, while for the TDTs flow rates between 0.02 and 0.2 L min^{-1} are recommended with a total sampling volume up to 4 L.

After sampling, TDTs are sealed with brass screw caps with PTFE ferrules and filters were kept between precleaned aluminum foil in separate sealed petri dishes. Both are stored at -18 °C in airtight containers until analysis.

2.5 Analysis method

Filters and TDTs were analyzed with TD-HR-ToF-CIMS (Aerodyne Research Inc., USA). Iodide served as the chemical ionization reagent which is selective for polar and oxidized organic compounds (Lee et al., 2014). The CIMS allows identification of individual compounds due to soft ionization as well as high-resolution mass spectra. The high sensitivity enables the analysis of small amounts of analyte, minimizing the necessary sample collection times (Aljawhary et al., 2013; Yatavelli et al., 2012).

For ionization, methyl-iodide from custom-made permeation tubes (permeation rate 450 ng/min at 30 °C) is diluted into dry nitrogen (purity 99.9999%), subsequently ionized by an alpha-polonium source (NRD Static Control, USA) to form iodide as reagent ion and inserted into the ion-molecular reaction chamber (IMR) at a flow rate of 2.2 L min^{-1}. For analysis, the filters were thermally desorbed into the IMR with heated dry nitrogen as carrier gas (purity 99.9999%, 1.9 L min^{-1}) using the FIGAERO-inlet (Lopez-Hilfiker et al., 2014); TDTs were desorbed with a flow rate of 0,120 L min^{-1} using a custom-built desorption unit. The temperature program for the carrier gas starts at 25 °C for 3 min, heating up to 200 °C with a rate of 17.5 °C min^{-1} and finally holding the temperature for 20 min. The reproducibility of the integrated ion signal intensity of different calibration compounds, determined through laboratory experiments, was found to be 10% for filter and 62% for TDT samples.

3 Characterization of the sampling system

3.1 Particle transport efficiency

The aerosol transport losses within the AERTRACC inlet and transport system were estimated with calculations using the Particle Loss Calculator (von der Weiden et al., 2009). The size-dependent transport losses were calculated based on the

geometry of the tubing system considering bends and non-vertical flows as well as volumetric flow rates (Fig. S4). Estimated
250 losses are below 10% for particles between 10 nm and 7 µm in diameter. For particles in the size-range 35 nm up to 3.5 µm,
where most of the collected particle mass is typically found, losses are below 2%. Applying the size-dependent losses to a
typical urban particle number size distribution, the overall calculated mass losses are below 1 %, both for PM_1 and PM_{10}.
Therefore, we conclude that particle transport losses within the sampling system are generally negligible for the mass-based
analysis methods and no correction for losses is needed.

255 **3.2 Time delay between aerosol measurement and sampling**

In *automatic operation mode*, the AERTRACC sampler is controlled based on the comparison of the specified sampling
conditions with the online-measured MoLa data. The difference of the volumetric flow rates between the online instrument
and the AERTRACC sampling inlets, which both have the same length and cross section, leads to different aerosol transport
times to the instruments and the sampling media, respectively. Due to the higher flow rate through the online instrument inlet
260 of 80 L min^{-1}, compared to 30 L min^{-1} (in PM_1/PM_{10} *sampling mode*) or 16.7 L min^{-1} (in PM_1-only *sampling mode*) through
the AIRTRACC inlet, the ambient aerosol reaches the online instruments before it reaches the sampling media. This
provides the opportunity of knowing in advance whether the aerosol reaching the sampling media should be sampled or not
and to switch the sampling valves accordingly.

To assure timely sampling of the targeted aerosols, it is necessary to know the time delay between the online measurement of
265 the aerosol and the aerosol reaching the sampling media. The time delay for each instrument is the time difference between
the times it takes for the aerosol from the moment it enters the inlet heads until the reporting by the online measurements,
and the aerosol reaching the sampling media, respectively.

Self-generated short spikes of elevated aerosol or trace gas concentrations were used to determine the time intervals between
the aerosol entering the inlet and the same aerosol being reported by each online instrument for different inlet heights (i.e.
270 3 m, 6 m, 9 m). These measurements showed that these time intervals can be separated into a transport-related residence time
in the inlet tubing and an instrument-specific measurement and reporting delay. The transport-related residence time was
extracted from the measurements with different inlet heights, since the instrument-specific measurement and reporting delay
is a constant for each instrument and independent of the inlet height. These measured transport times agree well with the
calculated transport times of the aerosol, based on tube cross sections and volumetric flow rates. This allows calculating the
275 respective transport times also for the sampling through the AERTRACC inlet without directly measuring it.

In the PM_1/PM_{10} *sampling mode* (i.e. with high sampling flow rate) in combination with short inlets of 3 m to 5 m above
ground level, for most instruments no delay time must be applied. For instruments with long measurement and reporting time
also no delay needs to be applied even for larger inlet heights.

The time delays for all instruments are implemented in the ACS software for the different inlet heights, which were specified
280 in the *flowrate* sub-window (Fig. 2b). For measurement variables, which are not associated with aerosol transport, like
meteorological data or GPS position, the respective instrument time delays are equal to the aerosol transport time through the

AERTRACC inlet. As example, the time delays for the 6 m inlet are 5-17 s for PM_1 *sampling mode* and 4-9 s for PM_1/PM_{10} *sampling mode,* excluding instruments with no time delay needed.

4 In-field validation of the AERTRACC using a single point source in a semi-urban environment

285 ### 4.1 Measurement setup

The AERTRACC sampler was tested and validated in the field by probing emissions from a wood-fired pizza oven, operated in a semi-urban environment. The goal was to sample the biomass burning emissions separately from the semi-urban background aerosol using the wind direction and further MoLa variables as sampling conditions. The test setup was located on the premises of the institute (Mainz, Germany), which is located at the outer edge of the city center, on the 21th July
290 2021. The oven was heated with logs of European beech and had a small chimney up to 4 m height above ground level. Larger roads were at a distance of 100 to 150 m, separated by a narrow row of trees and bushes from the measurement site. The main wind direction was northeast to east-northeast with one of the major roads and a fraction of the city upstream of the measurement site. MoLa with the installed AERTRACC sampler was located 13 m away from the pizza oven, in a direction that was frequently downwind of the source. Measurement and sampling inlets were at 4 m height above ground
295 level. Wind was very unstable during the measurement with air arriving temporarily from all directions at the measurement location. Regarding other meteorological parameters, it was a sunny day with few clouds; over the course of the measurement, the temperature was slightly rising from 21 °C to 24 °C while relative humidity decreased from 42% to 35%.

The pizza oven was heated up to 400 °C before pizza baking started. The whole measurement lasted for 3.5 h including 30 min of preparatory measurements to define sampling conditions for separate collection of source emissions and background
300 aerosol.

During the measurements, all MoLa instruments listed in Table 1 and in addition the HR-ToF-AMS with 15 s time resolution, in V-mode for maximum sensitivity (DeCarlo et al., 2006), were operated. For filter and TDT sampling the flow rates were set to 5 L min^{-1} and 0.12 L min^{-1}, respectively. Filter mass loading was limited to 2 µg and sampling time to 25 min to avoid overloading the filters and exceeding the breakthrough volume of the TDTs. As sampling conditions for the
305 pizza oven emissions, the wind sector 45-90° AND OPC particle number concentrations (PNC) >250 # cm^{-3} were chosen, while for background measurements the conditions were the wind sector 135-360° AND OPC PNC <200 # cm^{-3}. Two PM_{10} and two PM_1 filters and four TDTs were sampled with pizza oven emissions, and two filters, one for PM_{10} and PM_1 respectively, and two TDTs were sampled with background aerosol. For sampling media blank correction, two filters and TDTs each without sampling were taken as field blanks.

310 ### 4.2 Data Preparation and Analysis

The online data was quality checked, corrected for sampling delays and inspected for invalid data, e.g. data affected by internal calibration procedures, on a 1 s time base. Also, for the further data analysis, data with highest available time

resolution were used to be able to account for fast wind changes. PM_1 mass concentrations were calculated from combined FMPS and OPC size distribution data (details see Sect. S1). The high-resolution AMS data were analyzed with the software

315   SQUIRREL 1.63I and PIKA 1.23I. Furthermore, positive matrix factorization (PMF) (Paatero and Tapper, 1994) was applied on the organic particle fraction below m/z 116, measured with the AMS, using the PMF Evaluation Tool (PET) v3.07C (Ulbrich et al., 2009) to identify different aerosol types. Further details about AMS data processing and PMF are provided in the supplement Sect. S2. For analysis of the CIMS data, the software Tofware 3.2.3 (Aerodyne Inc., USA) and custom data procedures were used (details see Sect. S3). Signal intensity was normalized to the iodide-signal and sampled

320   volumes. Afterwards, the ions signal intensities were averaged over all available samples with pizza oven emissions and background, respectively, both for TDT and filter samples. Data for PM_1 and PM_{10} filter samples were handled and analyzed separately. The molecular formula of identified ions was determined for individual peaks and individual species were identified through the molecular formula and literature references (further details see Table S1).

4.3 Results and discussion

325   ### 4.3.1 Online measurements – characteristics of the measured aerosol

In the PMF analysis of the organic aerosol three aerosol types were identified, biomass burning organic aerosol (BBOA), cooking organic aerosol (COA) and oxygenated organic aerosol (OOA). Based on the individual PMF factor mass spectra and time series (see Fig. S1), this was the most reasonable PMF solution. Correlation of the obtained mass spectra with reference mass spectra resulted in average Pearson's r values of 0,86 for BBOA, 0,90 for COA and 0,92 for OOA (Fig. S3).

330   The BBOA mass spectrum shows the typical peaks at m/z 60 and 73, related to levoglucosan as typical biomass burning marker (Schneider et al., 2006). The OOA mass spectrum shows a strong peak for the key marker m/z 44 (CO_2^+) from thermal decarboxylation without any further distinct peaks at higher m/z (Ng et al., 2010). For COA no distinct markers exist, except for a high m/z 55 signal (Sun et al., 2011) and the identification was based on comparison with reference mass spectra from the HR-AMS Spectral Database (Ulbrich et al., 2022). The time series of BBOA and COA frequently showed

335   similar temporal variations indicating that they originate from the same source location while the OOA factor was mostly constant over the whole measurement interval and is representing the background aerosol. Further important time series, like PM_1 mass concentration and OPC particle number concentration, are shown in Fig. S5.

Because of the short measurement time and the close vicinity to the source, the temporal variations of aerosol and trace gas concentrations were mainly due to changes in wind directions and variations in emission strength of the targeted source

340   rather than to those of other sources or of atmospheric dilution. In Fig. 3a the concentrations of the three organic aerosol types, i.e. PMF factors, are shown as a function of the wind direction, averaged over 15° wind sectors. Further aerosol concentrations, which are assumed to be associated with the background and source emissions, are shown in Fig. 3b with suitable scaling factors to plot them together in a single polar graph. For BBOA and COA, a strong dependence of mass concentration on wind direction with a maximum for wind from the sector 60° to 90° was observed (Fig. 3a). A similar

345 dependence on wind direction was found for black carbon (BC) and polyaromatic hydrocarbons (PAH) (Fig. 3b), which are also likely associated with emissions from the pizza oven as well as BBOA and COA (Fachinger et al., 2017). OOA, as an indicator of background aerosol, is almost constant for all wind directions as well as sulfate (SO_4) which is often an indicator for secondary oxidized aerosol (Sun et al., 2011). These results show a clear enhancement of concentrations of aerosol components, which are related to the pizza oven emissions, when the wind was arriving from the direction of the source,

350 which was located in the direction of 70° with respect to the sampling location.
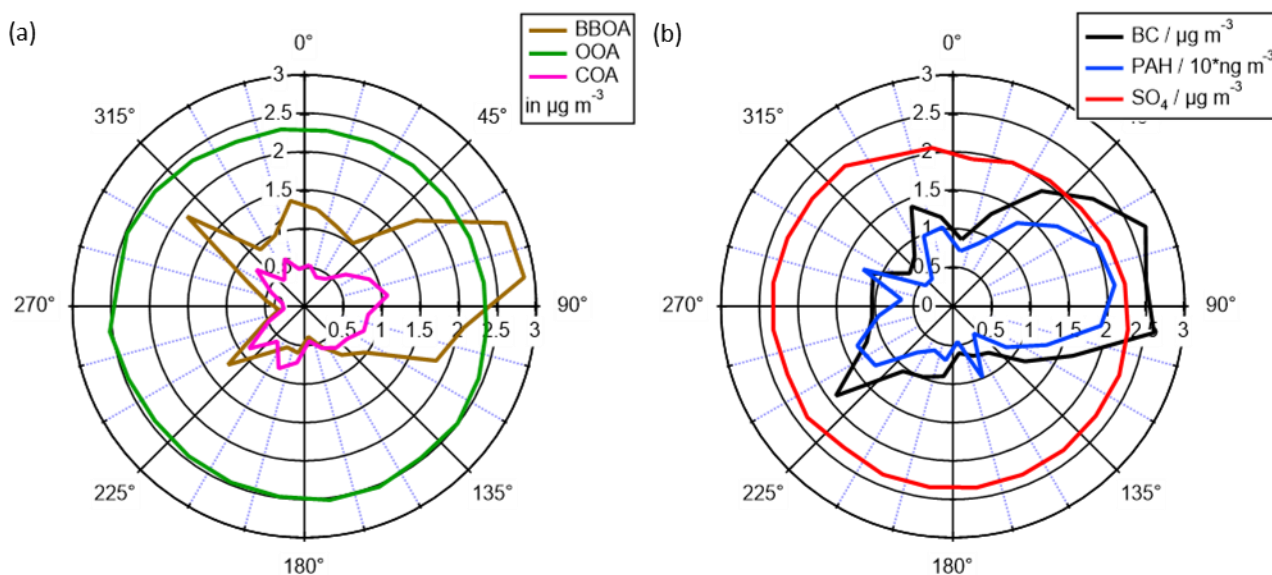
Figure 3: Concentrations of the organic aerosol types (a) as well as BC, PAH and SO_4 (b) dependent on local wind direction averaged over 15° sectors. The Pizza oven was located in the direction of 70° relative to MoLa.

4.3.2 Filter and TDT analysis

355 Source and background aerosol were separately sampled on filters and TDTs with sampling conditions based on preparatory measurements (see Sect. 4.1). The comparison of averaged signal intensities for identified ions from PM_1 and PM_{10} filter samples showed only negligible differences (Fig. S6), suggesting that most of the related aerosol mass is in the PM_1 particle size range. Therefore, the results are discussed for the PM_1 filters only.

For selected identified species, the ratio of the ion signal intensity from the pizza oven and the background samples was
360 calculated for the filter and the TDT samples (Fig. 4), respectively, to show which of the species mainly originate from background and which ones are associated with the source emissions. Additionally, the average ratio for all species assigned to only background (*aged/traffic*) and oven emissions (*biomass burning/cooking – BB/C*) as well as both groups (*mixed*) were calculated for comparison. The assignment to the sources must be regarded as a rather preliminary one, as the apportionment is only based on a literature review. The list of identified species and used acronyms is shown in Table 2 and
365 Table 3 for the filter and TDT samples, respectively. Substances found on the filters and TDTs differ mainly due to gas-
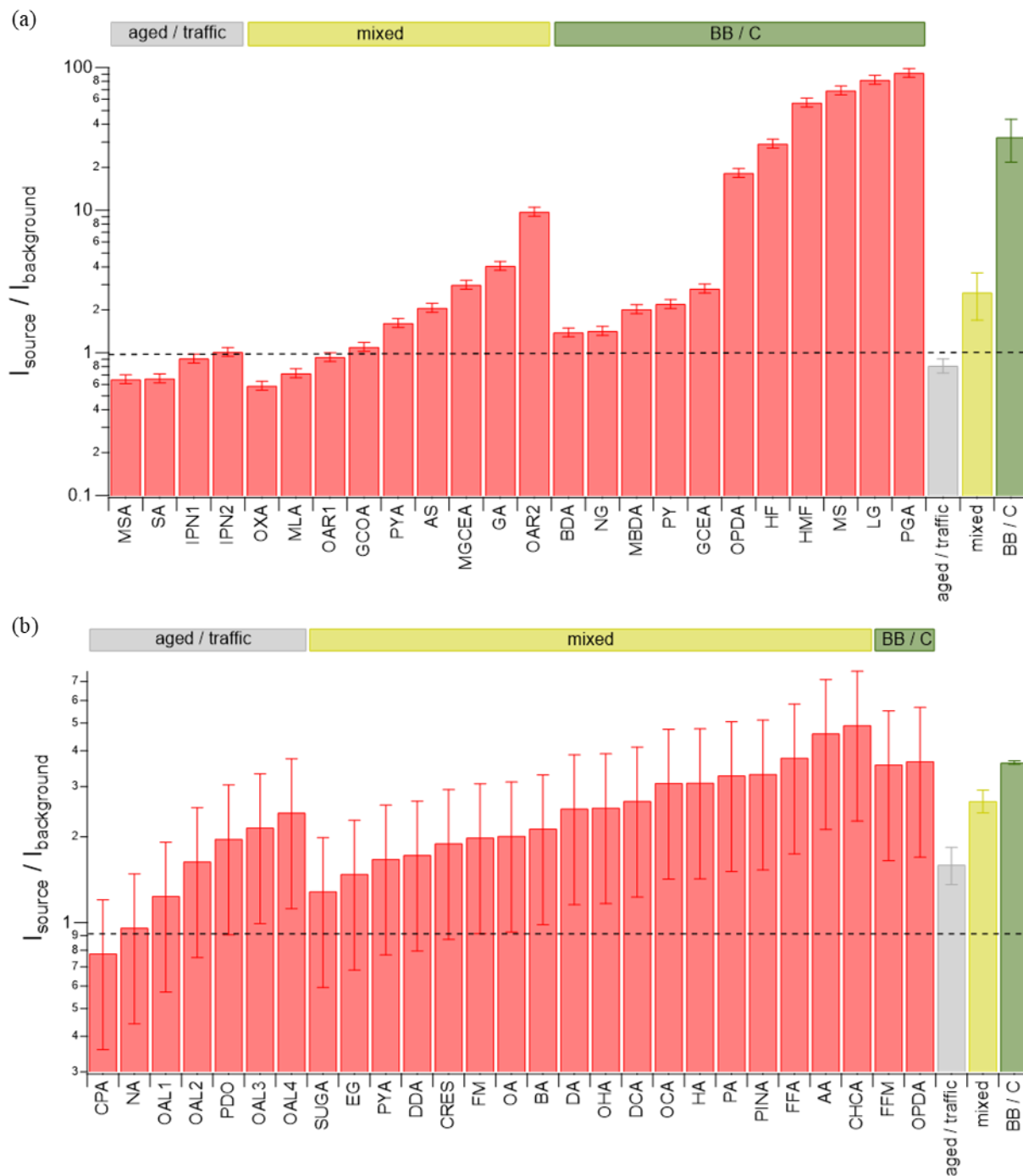
Figure 4: Ion signal intensity ratios of identified compounds from pizza oven and background for filter (a) and TDT (b) samples with source apportionment based on references (see Table S1 and S2). The dashed line represents a ratio of one, i.e. similar intensities found on pizza oven and background samples. The abbreviations *BB* and *C* stand for biomass burning and cooking. The errors bars result from an error propagation calculation for the standard error of the ion signal intensity, reproducibility, and the error obtained from the blank measurements (for details see Sect. S4).

370

particle partitioning and the selectivity of the TDT adsorbents. For some ions, based on the molecular formula, several substances are possible which are listed as well. Details like the exact *m/z* of the ions and references for source

375 apportionment of the species are summarized in Table S1 and S2. For species, which originate from background aerosol only, the ratio is expected to be in the order of one. They are typically associated with aged, oxidized aerosol or traffic emissions and should be found on the background and source samples in roughly equal amounts, after correcting for sampled volumes, since their origins are well distributed over all wind directions (see also Fig. 3, OOA aerosol). This is the case for the species found on the filter samples (Fig. 4a) that were assigned to traffic emissions or aged aerosol.

380 In contrast, identified compounds from the filter samples with source-to-background intensity ratios significantly larger than one are mostly known to be associated with biomass burning and cooking emissions, which is in good agreement with their higher abundance on the pizza oven-related filters. Compounds like levoglucosan (LG) and pyroglutaminic acid (PGA) which are markers for biomass burning and cooking, respectively, show more than 85 times higher intensities on the source-related filters compared to the background filters. In absolute concentrations, especially levoglucosan is dominant on these

385 filters with on average 73% of the total ion signal (reagent ion excluded).

Table 2: Selected identified compounds from filter analysis and acronyms used for Fig. 4a.

Acronym	Assigned compound	Acronym	Assigned compound
AS	ascorbic acid, hydroxyfurans	MLA	malic acid
BDA	butenedioic acid	MS	monosaccharide
GA	glutaric acid	MSA	methanesulfonic acid
GCEA	glyceric acid	NG	nitroguaiacol
GCOA	glycolic acid	OAR1	oxidized aromats, 3-acetylpentanedioic acid
HF/FA	hydroxy furfural, furoic acid	OAR2	oxidized aromats
HMF	hydroxymethyl furfural	ODPA	2-oxopropanedial, oxoacrylic acid
IPN1	oxidized isoprene nitrate	OXA	oxalic acid
IPN2	oxidized isoprene nitrate	PGA	pyroglutamic acid
LG	levoglucosan, galactosan, mannosan	PY	pyranose
MBDA	methylbutendioic acid	PYA	pyruvic acid
MGCEA	methylglyceric acid	SA	sulfuric acid

390

Table 3: Selected identified compounds from TDT analysis and acronyms used for Fig. 4b.

Acronym	Assigned compound	Acronym	Assigned compound
AA	acetic acid	OA	octanoic acid
BA	butyric acid, methyl propanoate	OAL1	oxidized alkyl
CHCA	cyclohexenecarboxylic acid	OAL2	oxidized alkyl
CPA	β-caryophyllene-aldehyde	OAL3	alkyldiole
CRES	cresol	OAL4	oxidized alkyl
DA	decanoic acid	OCA	oxocarboxylic acid
DCA	decenoic acid, pinanediol, linalool oxide	ODPA	oxopropanedial, oxoacrylic acid
DDA	dodecanoic acid, methylundecanoic acid	OHA	oxohexanoic acid, ethyl acetoacetate, methyloxopentanoic acid
EG	ethylene glycol	PA	propanoic acid
FFA	furfuryl alcohol, 2-furanmethanol	PDO	propandiol, hydroxyacetone
FFM	N-formylformamide, nitroethen	PINA	pinalic-3-acid
FM	formamide	PYA	pyruvic acid
HA	hexanoic acid, cyclopentanoic acid	SUGA	sugar acid
NA	nonenoic acid		

Some of those species, associated with cooking and biomass burning, can also originate from various other emission sources
395 and were assigned to the *mixed* group. They have a variety of different ratios between 0.6 and 10, showing that probably
some of them predominantly originate from the background aerosol while others mainly from the pizza oven emissions.
The large average source-to-background ratio for compounds attributed to biomass burning and cooking shows that the
targeted source emissions from the pizza oven were sampled predominantly on the source-related filters and not or only to a
small degree on the background filters. Compared to that the average ratios for the aged and traffic related compounds as
400 well as the *mixed* aerosol are considerably smaller indicating a clear separation of source-related emissions from
background-only aerosol using the selected AERTRACC sampling criteria.
From the TDT analysis, only two identified compounds were attributed solely to source-related emissions, i.e. cooking and
biomass burning, and both substances have ratios well above one as they probably originate from the pizza oven emissions
(Fig. 4b). The compounds assigned to traffic and aged aerosol have partially ratios in the order of one but also partially
405 significantly above one, i.e. they are present on source-related TDTs in larger amounts than on background-related TDTs.
Either these compounds are emitted by a close unknown source located in the same wind direction as the pizza oven or they
are emitted by the pizza oven as well and thus would belong to the mixed group. Most of the identified compounds from the

TDT samples can be assigned to different sources (*mixed*) having ratios which can be related to background aerosol and also to source related emissions.

410   Compared to the filter analysis the difference between average ratios of all source- and background-related compounds from the TDT analysis is smaller suggesting a weaker separation of source and background emissions. However, it must be taken into account that few compounds were assigned to only one of the aerosol types. As most of the compounds can originate from background as well as source-related emissions the enrichment of source-related compounds is smaller if these compounds are already present in the background aerosol. Thus, no specific markers were identified for the gas phase of the

415   pizza oven emissions, which would clearly show a very strong difference between background and source-related TDTs, in contrast to e.g. levoglucosan and pyroglutaminic acid on the filter samples.

In conclusion, for the filter samples the chosen sampling conditions for the background and source emissions proved to be suitable to sample the source emissions separately while the background emissions are found in approximately equal concentrations on the source and background filters at least based on the identified compounds. For the TDT samples the

420   shown ratios indicate a weaker separation of source and background emissions, likely because most of the identified compounds can originate from both, background and source emissions, and no distinct markers were found for the source emissions.

4.3.3 Evaluation of sampling conditions

The highly time-resolved MoLa online data provide the opportunity to post-evaluate the chosen AERTRACC sampling

425   conditions. This is done by comparing average source-related and background aerosol concentrations as well as total source-related sampling time for the chosen and other potential sampling conditions and by evaluating, whether a better separation between source emissions and background could herewith have been achieved. For the pizza oven measurement, the selected separation was based on a combination of PNC measured by OPC and wind direction (*Wind+OPC*), see Table 4 for details. For comparison, simpler conditions using only the wind direction (*Wind*) and stable wind conditions (*Wind stable*) were

430   evaluated. Stable wind conditions are fulfilled when wind from the source sector was observed at least for the previous 8 s, the transport time from the source to the MoLa inlet, which was calculated from the distance between the measurement inlet and the pizza oven, and the average wind speed during the measurements. Furthermore, the combination of PNC measured by CPC and wind direction was evaluated as additional sampling scenario (*Wind+CPC*).

To compare how well different sampling scenarios separate between source emissions and background, the mass

435   concentrations of black carbon (BC), polyaromatic hydrocarbons (PAH), organics measured by AMS, and PM_1 as well as PNC measured by CPC and OPC were used. These parameters were chosen as they showed to be strongly affected by the source emissions during the measurement, according to the online data analysis (Sect. 4.3.1).

Table 4: Sampling conditions for compared sampling scenarios for source and background sampling.

Sampling scenario	Source	Background
Wind	Wind direction 45-90°	Wind direction 135-360°
Wind stable	Wind direction 45-90° for 8 s	Wind direction 135-360° for 8 s
Wind + CPC	Wind direction 45-90° AND CPC PNC > 20,000 # cm^{-3}	Wind direction 135-360° AND CPC PNC < 15,000 # cm^{-3}
Wind + OPC	Wind direction 45-90° AND OPC PNC > 250 # cm^{-3}	Wind direction 135-360° AND OPC PNC < 200 # cm^{-3}

440

For assessment of source and background aerosol separation based on the various sampling scenarios, the ratios of averaged concentrations for "source" and "background" intervals, i.e. when the respective conditions were fulfilled, were calculated for each variable and each scenario (Fig. 5a). In addition, the potential sampling times that would have been spent to sample the source emissions and background aerosol for the various sampling scenarios, are shown in Fig. 5b.

445
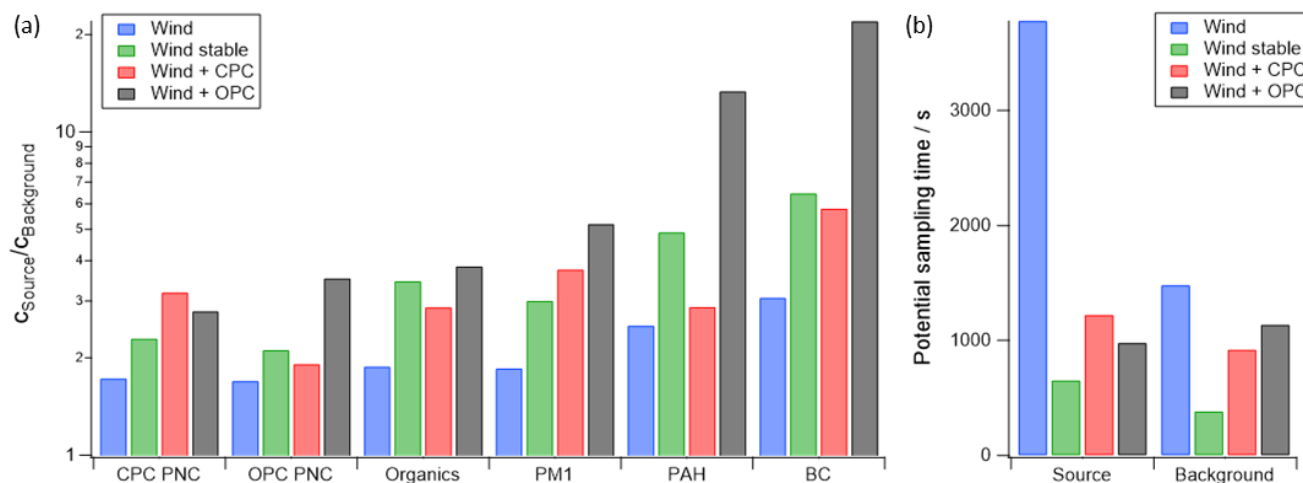
Figure 5: Ratio of averaged mass concentration and PNC of "source" and "background" aerosols, according the four different sampling scenarios (a), and related potential source emission and background aerosol sampling times (b).

450 Using only wind direction as separation criterion leads to the longest sampling times, especially for the source-related sampling. However, this approach also results in the smallest ratios of source versus background concentrations, i.e. the least effective separation of source emissions and background. Both effects are the result of the unspecific definition of the sampling condition. Due to fast wind changes, it is possible that source emissions miss the sampling inlet, which then

samples background or mixed aerosols, even though the "source" sampling criterion is fulfilled. Using stable wind
455 conditions as sampling scenario improves the separation substantially, but at the expense of sampling time, which is by far
the lowest for all four sampling scenarios.

The combination of elevated CPC PNC and the wind direction as sampling condition leads to higher ratios for measured
CPC PNC and PM$_1$ compared to the *Wind stable* sampling scenario, but similar or smaller ratios for the other parameters.
The sampling time is longer than for *Wind stable*, however still much lower than for the *Wind* sampling condition.

460 The largest ratios for almost all variables, and consequently the most effective separation of source-related and background
aerosol, were achieved when elevated PNC measured by OPC additional to the right wind direction were used as sampling
condition (*Wind+OPC*). This sampling scenario resulted in similar sampling time as the other "complex" sampling scenario
Wind+CPC and strongly improved sampling time, compared to the *Wind stable* scenario. Improved measurement of particle
mass-related variables like PM$_1$ or PAH mass concentration in this sampling scenario occurs, since the OPC counts the larger
465 particles (d_p = 0.25 µm – 32 µm) and therefore the OPC PNC represents the emitted mass concentration quite well. The
CPC, on the other hand, counts smaller particles (d_p = 5 nm – 3 µm); therefore, it captures better the total emitted PNC with
the very small particles contributing little to the emitted mass. Since for analysis of the sampling media, sampled particle
mass is the more relevant variable, compared to particle number, the *Wind+OPC* sampling scenario is better suited to control
the AERTRACC, compared to the *Wind+CPC* scenario. Contrary, in case of new particle formation events, the freshly
470 formed aerosol could be targeted using high CPC PNC and low PM$_1$ concentrations or low OPC PNC as sampling
conditions.

Long potential sampling times are desirable in order to quickly collect the necessary mass or sampling volume for analysis.
Therefore, for scenarios like *Wind stable*, longer overall measurement periods in the vicinity of the source are necessary to
reach sufficient sampled aerosol mass.

475 In an additional analysis, the choice of smaller wind sectors within the originally chosen wind sector 45-90° was evaluated to
investigate whether this could improve (i.e. enhance) the ratio between average source and background concentrations,
compared to the *Wind+OPC* scenario. The calculated ratios for all variables for the splitting of the original wind sectors into
three, five and seven sectors are shown in Table S3-S5. The split into three sectors improves the separation of source and
background emissions for the middle sector in comparison to the *Wind* scenario by at maximum 13 %. Further splitting leads
480 to partially improved ratios between source and background emissions by at maximum 20 % for five sectors and by at
maximum 22 % for seven sectors. However, the maximum values of ratios for different measured parameters spread over
several wind sectors and therefore does not point towards a "better" potential selection of the source wind sector. This spread
is probably due to indirect transport of the aerosol to the inlet due to frequently changing wind directions as well as due to
different time resolutions of the instruments. Additionally, with decreasing width of the wind sectors, the potential sampling
485 time per sector decreases for all sections leading to longer overall measurement times necessary to sample sufficient amounts
for subsequent analysis. Despite the improvement through smaller wind sectors, the ratios of the *Wind+OPC* scenario were
by far not reached, and the source-related sampling times were shorter for the 5- and 7-sector splitting, compared to the

Wind+OPC scenario. Consequently, using narrower wind sectors does not improve the separation of source and background emissions as effectively and as efficiently as choosing additional parameters to define the sampling conditions. In addition,

490 using only narrow wind sectors for separation of source-related and background aerosol requires very good knowledge about the wind direction for which the emission source is probed. This is not the case when wind direction is used in combination with other emission source-related features of the aerosol as sampling criterion. Therefore, in general, source-specific markers are needed, which are known and can be measured by MoLa, to define source-specific sampling conditions and to achieve the separate sampling of these emissions.

5 Summary

495

We developed the sampling system AERTRACC (AERosol and TRACe gas Collector) to separately sample the particulate and gas phase of source emissions and background aerosol in complex environments. It is incorporated in our mobile laboratory (MoLa) with its own inlet. Up to four samples can be taken in parallel, each onto a filter and a thermal desorption tube (TDT) for the particle and gas phase, respectively. Separation of different aerosols is achieved through external control

500 of the sampler based on online measurements of MoLa by setting suitable sampling conditions for the individual aerosols, which are compared with the online data. For this purpose, a self-programmed software is implemented in the MoLa data acquisition software for direct data access. For each of the four sampling paths up to four measured variables can be combined to create sampling conditions for the targeted aerosol, which are continuously compared with the current measured data. Besides the automatic sampling, the sampler can also be controlled manually.

505 The inlet and transport system was designed for minimal particle losses with typical estimated mass losses below 1 %. Due to shorter residence time of the aerosol in the MoLa online measurement inlet, compared to the sampling inlet, it can be analyzed with the online instruments and the sampling conditions are evaluated before the aerosol reaches the sampling media. These time delays were experimentally determined for all instruments and are considered in the AERTRACC control software.

510 For proof of concept and in-field validation, pizza oven emissions were probed in a semi-urban environment. The CIMS analysis of the hereby collected filters showed the successful separate sampling of source emissions from the background aerosol. Compounds known to be related to biomass burning and cooking were predominantly found on the source emissions filters while compounds associated with aged aerosol or traffic emissions were found in similar amounts on the background filters and the source emission filters. For gaseous species, the analysis of the TDTs indicate only a weak separation of

515 source and background emissions mainly because most of the identified species can originate from aged and traffic aerosol as well as from biomass burning and cooking emissions and no distinct markers were identified for the pizza oven emissions. Hence, these compounds can already be present in the background aerosol leading to a smaller increase in their concentrations due to source emissions.

The comparison of different potential sampling scenarios demonstrated the advantage of combining different measured variables to achieve targeted sampling of desired emissions. Using solely wind direction as sampling criterion, the separation was weak due to varying wind conditions leading to nonlinear aerosol transport. Adding source specific criteria like elevated particle number concentrations measured by the OPC improved the separation. As a consequence of this more effective separation of the emissions, the source apportionment of identified compounds is improved. An important requirement for AERTRACC to sample targeted aerosols is the knowledge about the source aerosol properties, which can be determined in preparatory measurements to define suitable sampling conditions for the different aerosols. Under such conditions, AERTRACC is capable to separate emissions of individual sources from those of other sources or from the aerosol background for improved chemical analysis of source-related emissions even in complex environments. Possible complex situations could be an industrial facility, like a steel plant, with different but closely located emission sources, e.g. coke oven, blast furnace, sinter plant, and traffic; or urban environments with emissions from traffic, wood combustion, and restaurants. Apart from TD-CIMS other analysis methods could be used to acquire the desired kinds of information from the samples. The TDTs can be analyzed with other thermal desorption methods, like TD-GC, while the filter samples can be analyzed with a broad spectrum of analytical methods.

Author contribution. JP and FD conceptualized the sampling system and field measurement. JP carried out the experiment, analyzed the MoLa data and prepared the paper with contributions from FD, LM und SB. LM developed the CIMS method and analyzed the samples using the developed method.

Competing interests. The authors declare that they have no conflict of interest.

Acknowledgements. We thank Thomas Böttger, Philipp Schuhmann, Antonis Dragoneas and the mechanical workshop for great support in the technical realization of the sampler. We also thank David Troglauer and Carsten Pallien for support during the in-field validation. Furthermore, we acknowledge the Max Planck Institute for Chemistry for funding of this work.

References

Aljawhary, D., Lee, A. K. Y., and Abbatt, J. P. D.: High-resolution chemical ionization mass spectrometry (ToF-CIMS): application to study SOA composition and processing, Atmos. Meas. Tech., 6, 3211–3224, https://doi.org/10.5194/amt-6-3211-2013, 2013.

Bai, Z., Ji, Y., Pi, Y., Yang, K., Wang, L., Zhang, Y., Zhai, Y., Yan, Z., and Han, X.: Hygroscopic analysis of individual Beijing haze aerosol particles by environmental scanning electron microscopy, Atmospheric Environment, 172, 149–156, https://doi.org/10.1016/j.atmosenv.2017.10.031, 2018.

Bhowmik, H. S., Shukla, A., Lalchandani, V., Dave, J., Rastogi, N., Kumar, M., Singh, V., and Tripathi, S. N.: Inter-comparison of online and offline methods for measuring ambient heavy and trace elements and water-soluble inorganic ions (NO_3^-, SO_4^{2-}, NH_4^+, and Cl^-) in $PM_{2.5}$ over a heavily polluted megacity, Delhi, Atmos. Meas. Tech., 15, 2667–2684, https://doi.org/10.5194/amt-15-2667-2022, 2022.

Canagaratna, M. R., Jayne, J. T., Jimenez, J. L., Allan, J. D., Alfarra, M. R., Zhang, Q., Onasch, T. B., Drewnick, F., Coe, H., Middlebrook, A., Delia, A., Williams, L. R., Trimborn, A. M., Northway, M. J., DeCarlo, P. F., Kolb, C. E., Davidovits, P., and Worsnop, D. R.: Chemical and microphysical characterization of ambient aerosols with the aerodyne aerosol mass spectrometer, Mass spectrometry reviews, 26, 185–222, https://doi.org/10.1002/mas.20115, 2007.

Celik, S., Drewnick, F., Fachinger, F., Brooks, J., Darbyshire, E., Coe, H., Paris, J.-D., Eger, P. G., Schuladen, J., Tadic, I., Friedrich, N., Dienhart, D., Hottmann, B., Fischer, H., Crowley, J. N., Harder, H., and Borrmann, S.: Influence of vessel characteristics and atmospheric processes on the gas and particle phase of ship emission plumes: in situ measurements in the Mediterranean Sea and around the Arabian Peninsula, Atmos. Chem. Phys., 20, 4713–4734, https://doi.org/10.5194/acp-20-4713-2020, 2020.

DeCarlo, P. F., Kimmel, J. R., Trimborn, A., Northway, M. J., Jayne, J. T., Aiken, A. C., Gonin, M., Fuhrer, K., Horvath, T., Docherty, K. S., Worsnop, D. R., and Jimenez, J. L.: Field-deployable, high-resolution, time-of-flight aerosol mass spectrometer, Analytical chemistry, 78, 8281–8289, https://doi.org/10.1021/ac061249n, 2006.

Dettmer, K. and Engewald, W.: Ambient air analysis of volatile organic compounds using adsorptive enrichment, Chromatographia, 57, S339-S347, https://doi.org/10.1007/BF02492126, 2003.

Dettmer, K. and Engewald, W.: Adsorbent materials commonly used in air analysis for adsorptive enrichment and thermal desorption of volatile organic compounds, Anal. Bioanal. Chem., 373, 490–500, https://doi.org/10.1007/s00216-002-1352-5, 2002.

Drewnick, F., Böttger, T., Weiden-Reinmüller, S.-L. von der, Zorn, S. R., Klimach, T., Schneider, J., and Borrmann, S.: Design of a mobile aerosol research laboratory and data processing tools for effective stationary and mobile field measurements, Atmos. Meas. Tech., 5, 1443–1457, https://doi.org/10.5194/amt-5-1443-2012, 2012.

Ebert, M., Weigel, R., Kandler, K., Günther, G., Molleker, S., Grooß, J.-U., Vogel, B., Weinbruch, S., and Borrmann, S.:
580   Chemical analysis of refractory stratospheric aerosol particles collected within the arctic vortex and inside polar
       stratospheric clouds, Atmos. Chem. Phys., 16, 8405–8421, https://doi.org/10.5194/acp-16-8405-2016, 2016.

Faber, P., Drewnick, F., Bierl, R., and Borrmann, S.: Complementary online aerosol mass spectrometry and offline FT-IR
       spectroscopy measurements: Prospects and challenges for the analysis of anthropogenic aerosol particle emissions,
       Atmospheric Environment, 166, 92–98, https://doi.org/10.1016/j.atmosenv.2017.07.014, 2017.

585 Fachinger, F., Drewnick, F., and Borrmann, S.: How villages contribute to their local air quality – The influence of traffic-
       and biomass combustion-related emissions assessed by mobile mappings of PM and its components, Atmospheric
       Environment, 263, 118648, https://doi.org/10.1016/j.atmosenv.2021.118648, 2021.

Fachinger, F., Drewnick, F., Gieré, R., and Borrmann, S.: How the user can influence particulate emissions from residential
       wood and pellet stoves: Emission factors for different fuels and burning conditions, Atmospheric Environment, 158,
590   216–226, https://doi.org/10.1016/j.atmosenv.2017.03.027, 2017.

Forbes, P.: Atmospheric Chemistry Analysis: A Review, Analytical chemistry, 92, 455–472,
       https://doi.org/10.1021/acs.analchem.9b04623, 2020.

Fuzzi, S., Baltensperger, U., Carslaw, K., Decesari, S., van der Denier Gon, H., Facchini, M. C., Fowler, D., Koren, I.,
       Langford, B., Lohmann, U., Nemitz, E., Pandis, S., Riipinen, I., Rudich, Y., Schaap, M., Slowik, J. G., Spracklen, D. V.,
595   Vignati, E., Wild, M., Williams, M., and Gilardoni, S.: Particulate matter, air quality and climate: lessons learned and
       future needs, Atmos. Chem. Phys., 15, 8217–8299, https://doi.org/10.5194/acp-15-8217-2015, 2015.

Gilardoni, S.: Advances in organic aerosol characterization: From complex to simple, Aerosol Air Qual. Res., 17, 1447–
       1451, https://doi.org/10.4209/aaqr.2017.01.0007, 2017.

Gordon, H., Kirkby, J., Baltensperger, U., Bianchi, F., Breitenlechner, M., Curtius, J., Dias, A., Dommen, J., Donahue, N.
600   M., Dunne, E. M., Duplissy, J., Ehrhart, S., Flagan, R. C., Frege, C., Fuchs, C., Hansel, A., Hoyle, C. R., Kulmala, M.,
       Kürten, A., Lehtipalo, K., Makhmutov, V., Molteni, U., Rissanen, M. P., Stozkhov, Y., Tröstl, J., Tsagkogeorgas, G.,
       Wagner, R., Williamson, C., Wimmer, D., Winkler, P. M., Yan, C., and Carslaw, K. S.: Causes and importance of new
       particle formation in the present-day and preindustrial atmospheres, J. Geophys. Res., 122, 8739–8760,
       https://doi.org/10.1002/2017JD026844, 2017.

605 Hallquist, M., Wenger, J. C., Baltensperger, U., Rudich, Y., Simpson, D., Claeys, M., Dommen, J., Donahue, N. M., George,
       C., Goldstein, A. H., Hamilton, J. F., Herrmann, H., Hoffmann, T., Iinuma, Y., Jang, M., Jenkin, M. E., Jimenez, J. L.,
       Kiendler-Scharr, A., Maenhaut, W., McFiggans, G., Mentel, T. F., Monod, A., Prévôt, A. S. H., Seinfeld, J. H., Surratt,
       J. D., Szmigielski, R., and Wildt, J.: The formation, properties and impact of secondary organic aerosol: current and
       emerging issues, Atmos. Chem. Phys., 9, 5155–5236, https://doi.org/10.5194/acp-9-5155-2009, 2009.

610 Harper, M.: Sorbent trapping of volatile organic compounds from air, J. Chromatogr. A, 885, 129–151,
       https://doi.org/10.1016/S0021-9673(00)00363-0, 2000.

Heard, D. E.: Analytical techniques for atmospheric measurement, Blackwell Pub, Ames, Iowa, 510 pp., 2006.

Johnston, M. V. and Kerecman, D. E.: Molecular Characterization of Atmospheric Organic Aerosol by Mass Spectrometry, Annual review of analytical chemistry (Palo Alto, Calif.), 12, 247–274, https://doi.org/10.1146/annurev-anchem-061516-045135, 2019.

Laskin, J., Laskin, A., and Nizkorodov, S. A.: Mass Spectrometry Analysis in Atmospheric Chemistry, Analytical chemistry, 90, 166–189, https://doi.org/10.1021/acs.analchem.7b04249, 2018.

Lee, B. H., Lopez-Hilfiker, F. D., Mohr, C., Kurtén, T., Worsnop, D. R., and Thornton, J. A.: An iodide-adduct high-resolution time-of-flight chemical-ionization mass spectrometer: application to atmospheric inorganic and organic compounds, Environmental science & technology, 48, 6309–6317, https://doi.org/10.1021/es500362a, 2014.

Lopez-Hilfiker, F. D., Mohr, C., Ehn, M., Rubach, F., Kleist, E., Wildt, J., Mentel, T. F., Lutz, A., Hallquist, M., Worsnop, D., and Thornton, J. A.: A novel method for online analysis of gas and particle composition: description and evaluation of a Filter Inlet for Gases and AEROsols (FIGAERO), Atmos. Meas. Tech., 7, 983–1001, https://doi.org/10.5194/amt-7-983-2014, 2014.

Mercier, F., Glorennec, P., Blanchard, O., and Le Bot, B.: Analysis of semi-volatile organic compounds in indoor suspended particulate matter by thermal desorption coupled with gas chromatography/mass spectrometry, Journal of chromatography. A, 1254, 107–114, https://doi.org/10.1016/j.chroma.2012.07.025, 2012.

Ng, N. L., Canagaratna, M. R., Zhang, Q., Jimenez, J. L., Tian, J., Ulbrich, I. M., Kroll, J. H., Docherty, K. S., Chhabra, P. S., Bahreini, R., Murphy, S. M., Seinfeld, J. H., Hildebrandt, L., Donahue, N. M., DeCarlo, P. F., Lanz, V. A., Prévôt, A. S. H., Dinar, E., Rudich, Y., and Worsnop, D. R.: Organic aerosol components observed in Northern Hemispheric datasets from Aerosol Mass Spectrometry, Atmos. Chem. Phys., 10, 4625–4641, https://doi.org/10.5194/acp-10-4625-2010, 2010.

Paatero, P. and Tapper, U.: Positive matrix factorization: A non-negative factor model with optimal utilization of error estimates of data values, Environmetrics, 5, 111–126, https://doi.org/10.1002/env.3170050203, 1994.

Parshintsev, J. and Hyötyläinen, T.: Methods for characterization of organic compounds in atmospheric aerosol particles, Anal. Bioanal. Chem., 407, 5877–5897, https://doi.org/10.1007/s00216-014-8394-3, 2015.

Schneider, J., Weimer, S., Drewnick, F., Borrmann, S., Helas, G., Gwaze, P., Schmid, O., Andreae, M. O., and Kirchner, U.: Mass spectrometric analysis and aerodynamic properties of various types of combustion-related aerosol particles, International Journal of Mass Spectrometry, 258, 37–49, https://doi.org/10.1016/j.ijms.2006.07.008, 2006.

Shrivastava, M., Cappa, C. D., Fan, J., Goldstein, A. H., Guenther, A. B., Jimenez, J. L., Kuang, C., Laskin, A., Martin, S. T., Ng, N. L., Petaja, T., Pierce, J. R., Rasch, P. J., Roldin, P., Seinfeld, J. H., Shilling, J., Smith, J. N., Thornton, J. A., Volkamer, R., Wang, J., Worsnop, D. R., Zaveri, R. A., Zelenyuk, A., and Zhang, Q.: Recent advances in understanding secondary organic aerosol: Implications for global climate forcing, Rev. Geophys., 55, 509–559, https://doi.org/10.1002/2016RG000540, 2017.

Stavroulas, I., Bougiatioti, A., Grivas, G., Paraskevopoulou, D., Tsagkaraki, M., Zarmpas, P., Liakakou, E., Gerasopoulos, E., and Mihalopoulos, N.: Sources and processes that control the submicron organic aerosol composition in an urban

Mediterranean environment (Athens): a high temporal-resolution chemical composition measurement study, Atmos. Chem. Phys., 19, 901–919, https://doi.org/10.5194/acp-19-901-2019, 2019.

Struckmeier, C., Drewnick, F., Fachinger, F., Gobbi, G. P., and Borrmann, S.: Atmospheric aerosols in Rome, Italy: sources, dynamics and spatial variations during two seasons, Atmos. Chem. Phys., 16, 15277–15299, https://doi.org/10.5194/acp-16-15277-2016, 2016.

Sun, Y.-L., Zhang, Q., Schwab, J. J., Demerjian, K. L., Chen, W.-N., Bae, M.-S., Hung, H.-M., Hogrefe, O., Frank, B., Rattigan, O. V., and Lin, Y.-C.: Characterization of the sources and processes of organic and inorganic aerosols in New York city with a high-resolution time-of-flight aerosol mass apectrometer, Atmos. Chem. Phys., 11, 1581–1602, https://doi.org/10.5194/acp-11-1581-2011, 2011.

Ulbrich, I. M., Handschy, A., Lechner, M., and Jimenez, J.L.: High-Resolution AMS Spectral Database, 2022. Last access: 21.04.2022.

Ulbrich, I. M., Canagaratna, M. R., Zhang, Q., Worsnop, D. R., and Jimenez, J. L.: Interpretation of organic components from Positive Matrix Factorization of aerosol mass spectrometric data, Atmos. Chem. Phys., 9, 2891–2918, https://doi.org/10.5194/acp-9-2891-2009, 2009.

von der Weiden, S.-L., Drewnick, F., and Borrmann, S.: Particle Loss Calculator – a new software tool for the assessment of the performance of aerosol inlet systems, Atmos. Meas. Tech., 2, 479–494, https://doi.org/10.5194/amt-2-479-2009, 2009.

Williams, B. J., Goldstein, A. H., Kreisberg, N. M., and Hering, S. V.: An In-Situ Instrument for Speciated Organic Composition of Atmospheric Aerosols: Thermal Desorption Aerosol GC/MS-FID (TAG), Aerosol Sci. Technol., 40, 627–638, https://doi.org/10.1080/02786820600754631, 2006.

Woolfenden, E.: Sorbent-based sampling methods for volatile and semi-volatile organic compounds in air. Part 2. Sorbent selection and other aspects of optimizing air monitoring methods, J. Chromatogr. A, 1217, 2685–2694, https://doi.org/10.1016/j.chroma.2010.01.015, 2010.

Yatavelli, R. L. N., Lopez-Hilfiker, F., Wargo, J. D., Kimmel, J. R., Cubison, M. J., Bertram, T. H., Jimenez, J. L., Gonin, M., Worsnop, D. R., and Thornton, J. A.: A Chemical Ionization High-Resolution Time-of-Flight Mass Spectrometer Coupled to a Micro Orifice Volatilization Impactor (MOVI-HRToF-CIMS) for Analysis of Gas and Particle-Phase Organic Species, Aerosol Science and Technology, 46, 1313–1327, https://doi.org/10.1080/02786826.2012.712236, 2012.

Zhou, W., Xu, W., Kim, H., Zhang, Q., Fu, P., Worsnop, D. R., and Sun, Y.: A review of aerosol chemistry in Asia: insights from aerosol mass spectrometer measurements, Environmental science. Processes & impacts, 22, 1616–1653, https://doi.org/10.1039/D0EM00212G, 2020.

Zhou, Y., Huang, X. H., Bian, Q., Griffith, S. M., Louie, P. K. K., and Yu, J. Z.: Sources and atmospheric processes impacting oxalate at a suburban coastal site in Hong Kong: Insights inferred from 1 year hourly measurements, J. Geophys. Res., 120, 9772–9788, https://doi.org/10.1002/2015JD023531, 2015.